OPEN

PRS GLOBAL OPEN

EXPERIMENTAL

Squid Ring Teeth–coated Mesh Improves Abdominal Wall Repair

Ashley N. Leberfinger, MD*
Monika Hospodiuk, MS†
Abdon Pena-Francesch, PhD‡
Bugra Ayan, MS†
Veli Ozbolat, PhD†
Srinivas V. Koduru, PhD*
Ibrahim T. Ozbolat, PhD†‡§
Melik C. Demirel, PhD†‡§¶
Dino J. Ravnic, DO, MPH*

Background: Hernia repair is a common surgical procedure with polypropylene (PP) mesh being the standard material for correction because of its durability. However, complications such as seroma and pain are common, and repair failures still approach 15% secondary to poor tissue integration. In an effort to enhance mesh integration, we evaluated the applicability of a squid ring teeth (SRT) protein coating for soft-tissue repair in an abdominal wall defect model. SRT is a biologically derived high-strength protein with strong mechanical properties. We assessed tissue integration, strength, and biocompatibility of a SRT-coated PP mesh in a first-time pilot animal study.

Methods: PP mesh was coated with SRT (SRT-PP) and tested for mechanical strength against uncoated PP mesh. Cell proliferation and adhesion studies were performed in vitro using a 3T3 cell line. Rats underwent either PP (n = 3) or SRT-PP (n = 6) bridge mesh implantation in an anterior abdominal wall defect model. Repair was assessed clinically and radiographically, with integration evaluated by histology and mechanical testing at 60 days.

Results: Cell proliferation was enhanced on SRT-PP mesh. This was corroborated in vivo by abdominal wall histology, dramatically diminished craniocaudal mesh contraction, improved strength testing, and higher tissue failure strain. There was no increase in seroma or visceral adhesion formation. No foreign body reactions were noted on liver histology.

Conclusions: SRT applied as a coating appears to augment mesh–tissue integration and improve abdominal wall stability following bridged repair. Further studies in larger animals will determine its applicability for hernia repair in patients. *(Plast Reconstr Surg Glob Open 2018;6:e1881; doi: 10.1097/GOX.0000000000001881; Published online 7 August 2018.)*

INTRODUCTION

Hernia repair is one of the most common surgical procedures worldwide.[1] Approximately 400,000 procedures are performed in the United States annually with associated costs exceeding 3 billion dollars.[2] Hernias can be associated with pain, discomfort, and weakness.[3] Furthermore, they can result in intestinal obstruction and strangulation requiring emergency surgery, leading to associated morbidity and mortality.[4]

Reparative surgery utilizing mesh for abdominal wall repair is often indicated, especially in complicated hernia repairs.[5] It is estimated that one third of patients with a recurrent ventral hernia repair experience an additional failure, and with each subsequent repair, there is a stepwise worsening of long-term outcomes.[6] Because Usher widely introduced a plastic prosthesis for hernia repair in 1955, nonabsorbable synthetic mesh, such as polypro-

*From the *Department of Surgery, Penn State University College of Medicine, Hershey, Pa.; †Department of Engineering Science and Mechanics, Penn State University, University Park, Pa.; ‡Department of Biomedical Engineering, Penn State University, University Park, Pa.; §The Huck Institutes of Life Sciences, Penn State University, University Park, Pa.; and ¶Materials Research Institute, Penn State University, University Park, Pa.*

Received for publication April 12, 2018; accepted June 8, 2018.

Supported by Army Research Office under grant No. W911NF-16-1-0019 (MCD).

DOI: 10.1097/GOX.0000000000001881

Disclosure: *Melik C. Demirel and Abdon Pena-Francesch have a pending patent application on SRT proteins. Neither of the other authors has no financial interest to declare in relation to the content of this article. The Article Processing Charge was paid for by the authors.*

Supplemental digital content is available for this article. Clickable URL citations appear in the text.

pylene (PP), has become widespread.[7] However, its intraperitoneal use has been questioned since Kaufman et al.[8] first documented fistula formation in 1981 and has led to legal concerns more recently.[9] This has led to the development of biologic and composite mesh, especially for use in patients where an overlay or sublay repair cannot be performed and the implanted material is in direct contact with the viscera. The average cost of a biologic mesh repair exceeds $85,000 per patient[10] with recurrence rates >30%.[11] Therefore, a major challenge is to develop an affordable material, which can be utilized for strong and definitive repair when fascial reapproximation is not possible and a bridged technique is required.

Our unique solution to this problem is a structural protein, which offers high strength, biocompatibility, and low production costs. Repetitive structural proteins such as squid ring teeth (SRT) protein have mechanical properties that exceed most natural and synthetic polymers.[12] They offer unique characteristics such as reversible assembly of their physically cross-linked molecular structures, and ultra-high energy absorbance, elasticity, and toughness (capacity of a material to absorb energy and deform up to the point of mechanical failure).[13] Our previous work on SRT has received attention for its thermoplasticity and self-healing characteristics.[14,15] However, SRT has never been used in animal studies. The objective of this pilot study was to evaluate the applicability of SRT protein for soft-tissue repair in an abdominal wall defect model. We hypothesized that SRT would offer superior abdominal wall integration and strength when used as a coating compared with standard PP mesh.

MATERIALS AND METHODS

Fabrication and Characterization

Squid ring teeth were extracted from suction cups in the arms and tentacles of *Loligo pealeii* squid (**see figure, Supplemental Digital Content 1a–c, which displays SRT protein, *http://links.lww.com/PRSGO/A827***). The rings are composed of proteins ranging from 15 to 60 kDa (**Supplemental Digital Content 1d**). SRT samples were washed in water and ethanol and then dried in ambient conditions. They were dissolved overnight in 1,1,1,3,3,3-Hexafluoro-2-propanol to a concentration of 50 mg/mL and purified by centrifugation. Large pore monofilament PP mesh (Bard; ref# 0112680; New Providence, N.J.) was cut into 2×5 cm strips and dip coated with SRT/1,1,1,3,3,3-Hexafluoro-2-propanol solution (**Supplemental Digital Content 1e**). Coated strips were dried at room temperature and washed in deionized water. The resulting SRT-coated PP mesh strips (SRT-PP) had 15% ± 5% of protein content (w/w). Spectral data were collected (Thermo Nicolet IR) under attenuated total reflection (ATR, diamond crystal) mode using Norton–Beer apodization with 4 cm^{-1} resolutions. For each spectrum, 256 scans were coadded. Uniaxial tensile testing of SRT-PP and uncoated PP mesh (control) was performed in a TA 800Q DMA instrument. Thin film fixtures were used to clamp the specimens, and strain ramp measurements were performed at a strain rate of 5%/min.

Cell Preparation and Adhesion Assay

3T3 fibroblasts (ATCC, Manassas, Va.) were cultured in Dulbecco's modified eagle's medium (Corning Cellgro; Manassas, Va.) supplemented with 10% fetal bovine serum (FBS) (Life Technologies, Grand Island, N.Y.), 100 U/mL Penicillin G, and 100 µg/mL streptomycin (Life Technologies). Cells were maintained at 37°C in 5% CO_2. Meshes were soaked in 70% ethanol for 5 minutes and washed in phosphate-buffered saline, then 3T3 media, and placed into individual wells of a 24 well plate. Cells were seeded at a concentration of 2×10^6 in 300 µL 3T3 media. Plates were incubated for 6 hours; then an additional 150 µL of media was added and incubated overnight. Mesh was transferred to new wells in a cell-repellent plate. Culture medium was changed every 2 days over a 7-day period. Meshes were imaged with an EVOS FL Auto inverted microscope (ThermoFisher, Pittsburgh, Pa.). They were then stained to determine adhesion at 3 time points (1, 4, and 7 d). At each time point, 3 SRT-PP and PP meshes were rinsed with Dulbecco's phosphate buffered saline (DPBS; Life Technologies). Four hundred microliter of DPBS with 2 µM calcein-AM (Invitrogen, Carlsbad, Calif.) and 4 µM ethidium homodimer (Life Technologies) was added. Plates were protected from light and incubated for 30 minutes and then rinsed again. Four representative areas of each mesh were randomly selected for imaging. Adhesion was quantified using ImageJ (National Institutes of Health, Bethesda, Md.). After 7 days of culture, meshes were fixed overnight with 4% paraformaldehyde (Sigma-Aldrich; St. Louis, Mo.) at 4°C. Constructs were washed in DPBS. Permeabilization was performed with 0.25% Triton X-100 (Sigma-Aldrich) and 1% bovine serum albumin (RPI Corp., Mount Prospect, Ill.) diluted in DPBS and incubated for 1 hour. Meshes were double stained with Alexa Fluor 568 Phalloidin 1:100 and 5 µg/mL 4′,6-diamidino-2-phenylindole DAPI. Samples were washed and imaged on a confocal laser scanning microscope (Olympus FV10i; Tokyo, Japan).

Scanning Electron Microscopy

Field emission scanning electron microscopy (Nova NanoSEM 630; FEI, Hillsboro, Ore.) was used to investigate surface topography. Meshes were fixed overnight with 4% paraformaldehyde (Sigma-Aldrich) at 4°C. Constructs were washed in DPBS and dehydrated using graded ethanol solutions (25–100%). Meshes were further dried in a critical point dryer (CPD300; Leica EM; Wetzlar, Germany), sputter coated with iridium (K557X Emitech Sputter Coater, Tex.) and observed at an accelerating voltage of 10 keV.

Vertebrate Animal Procedures

Animals were monitored and cared for by the Department of Comparative Medicine, and studies were performed in AAALAC-accredited facilities. Veterinary care was administered in accordance with guidelines in The Guide for Care and Use of Laboratory Animals, 8th edition.

In Vivo Implantation

Anesthesia and postoperative analgesia were administered under Penn State institutional animal protocol

#47197. Nine 10-week-old Sprague Dawley rats (4 male and 5 female) were anesthetized with inhalational isoflurane and a subcutaneous injection of carprofen (5 mg/kg) was administered. A warm water blanket was used to prevent excessive heat loss and a sterile surgical field was created. Ethylene oxide was used for mesh sterilization. A 2×5 cm full-thickness segment of anterior abdominal wall was excised to allow for mesh placement. The fascia and muscle layers were repaired with a bridging technique (no mesh overlap with muscle). After randomization, 3 males and 3 females received SRT-PP mesh, whereas 2 females and 1 male received PP mesh. Mesh was secured using 4-0 monocryl sutures in an interrupted fashion, and the overlying skin was closed with subcuticular 4-0 monocryl. Postoperatively, animals were examined daily for the first week and then three times per week thereafter for weight loss, pain, hernia development, or other complications.

In Vivo Magnetic Resonance Imaging

At day 60, animals underwent magnetic resonance imaging (MRI). Inhalational isoflurane was used for anesthesia. Animals were placed inside a holder (Acrylic Glass animal cradle equipped with a nosecone and adjustable bite bar) and then into the MRI (7-Tesla 300MHz 70/20as Bruker Biospec MRI system; Bruker Biospin, Ettlingen, Germany). A respiration monitor (PC-SAM Model 1025; SA Instruments, Stony Brook, N.Y.) was used, and isoflurane was adjusted in response to monitored breaths per minute. After the initial localizer scan was performed, a 2D T2-weighted scan rapid acquisition with relaxation enhancement (RARE) was acquired with the following parameters: TR/TE = 4101/12.0 ms, 8 averages, 1 echo, 256×256 matrix, 6.0×6.0 cm FOV, RARE factor = 8, and slice thickness 1 mm (40 slices). Total acquisition time of the scan (respiratory-gated) was approximately 30 minutes. Immediately after MRI, anesthetized animals were sacrificed. Image analysis was conducted using ImageJ.

Histology

The anterior abdominal wall was opened widely along 3 sides of the mesh allowing for hinged exposure of the intra-abdominal contents. Digital photographs were taken and adhesions were scored macroscopically by 2 blinded observers using a 5-point scoring system that accounted for extent (percentage of mesh involved), type (flimsy or dense), and tenacity (how difficult to dislodge) as previously described.[16] A 3 cm rim of surrounding abdominal wall was excised along with the mesh. Two specimens from each rat were prepared for histological analysis. Tissue was fixed with 10% formalin, processed in paraffin, sectioned, and stained with either hematoxylin and eosin (H&E) or Masson's trichrome. Slides were scored for inflammatory cell infiltrates, neovascularization, necrosis, and hemorrhage as previously described.[16] A section of liver was also prepared for H&E staining.

Biomechanical Testing of Explants

Mesh specimens were prepared as 1 cm wide by 5 cm long (3 cm abdominal wall and 2 cm mesh) strips and placed in 0.9% sodium chloride. An Instron 5966 tensile testing device (Norwood, Mass.) was used to perform uniaxial tensile testing. The specimens were fixed on upper and lower gripers using metal sutures and rigidly held by a 1 kN load-cell platform. The lower gripper held the tissue and the upper gripper held the mesh side of the explant. Specimens were manually loaded until positive tension was reached. The length of the reduced section was measured, and tensile loads were applied at a loading rate of 500 mm/min until failure was observed. Tensile stress, strain, peak stress, and strain at break were recorded.

Statistical Analysis

Student's t test was used to compare paired results with $P < 0.05$ considered statistically significant.

RESULTS

In vitro results showed that the composite SRT mesh has strong mechanical properties. In vivo implantation showed SRT-PP mesh to be biocompatible and having superior tissue integration compared with the uncoated control. We chose rats for this pilot study because they represented the smallest accepted animal model for abdominal wall repair.

In Vitro Testing of SRT Mesh

Mesh thickness, measured with a micrometer, was slightly increased after SRT coating (70–92 μm; Fig. 1A, B). Coating was verified by Fourier-transform infrared spectroscopy. Fourier-transform infrared spectroscopy spectrum of PP mesh showed characteristic absorption bands of PP (Fig. 1C).[17] SRT showed bands characteristic of proteins or polyamides.[18] SRT-PP mesh showed absorption bands from both PP and SRT, indicating coating was successful. Mechanical comparisons were then made between the 2 groups. PP mesh showed a linear response with strain until failure at 50% strain (unweaving at the edges) at a tensile stress of 2.0±0.5 MPa (Fig. 1D). However, composite SRT-PP mesh showed a clear increase in the tensile load for the same deformation (increase of 6 N), followed by a linear region similar to the PP mesh (tensile stress of 3.6±0.7 MPa).

Cell Seeding, Count, and Adhesion

3T3 cells accumulated within the woven areas of the mesh. Cell density on SRT-PP mesh increased significantly over time and more than 3-fold by day 7 (8.17 cells/mm^2 on day 1, 13.02 cells/mm^2 on day 4, and 29.99 cells/mm^2 on day 7), whereas the density on control mesh remained relatively unchanged (around 8 cells/mm^2; Fig. 2A). The difference between cell content is shown on the confocal images (**Supplemental Digital Content 2**), where cells on composite SRT-PP mesh demonstrated increased fluorescent intensity compared with PP mesh (Fig. 2B, C) (**see figure, Supplemental Digital Content 2, which displays SEM, *http://links.lww.com/PRSGO/A828***).

In Vivo Implantation and Radiographic Evaluation

In our studies, all rats had appropriate weight gain and no systemic signs of distress after implantation, indicating biocompatibility of the material. We did not observe

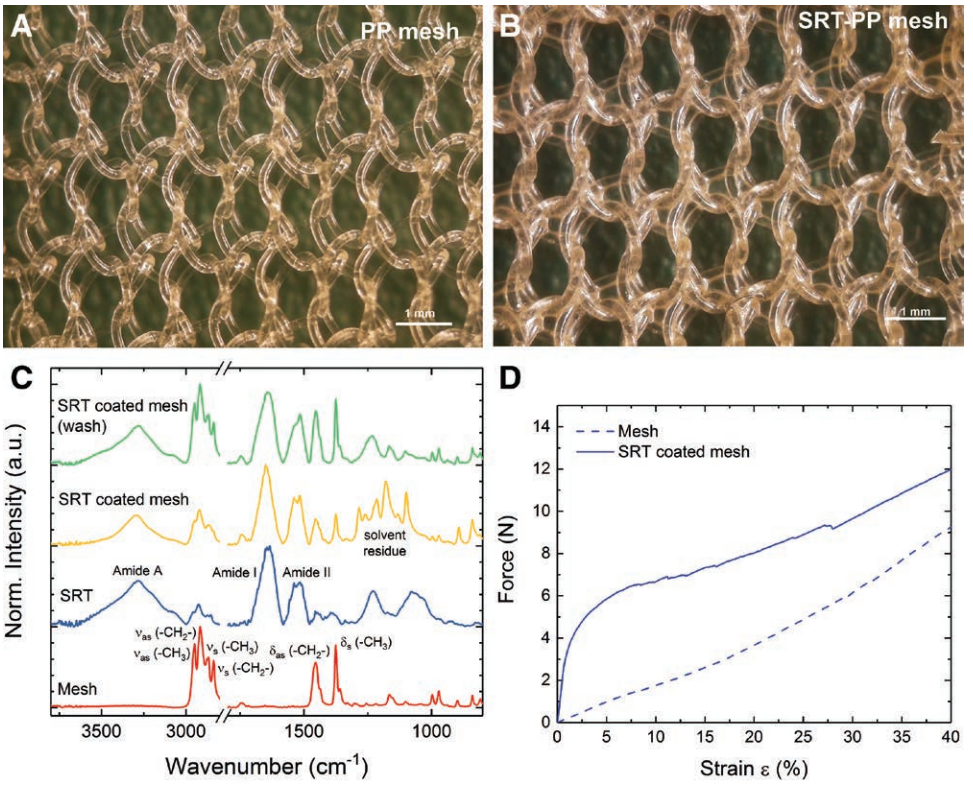

Fig. 1. In vitro testing of SRT mesh. A, Uncoated PP mesh. B, Composite SRT-PP mesh after coating. C, Fourier-transform infrared spectroscopy spectrum of PP mesh, SRT protein, composite SRT-PP mesh, and composite SRT-PP mesh after washing. D, Uniaxial tensile testing of composite SRT-PP and control PP mesh.

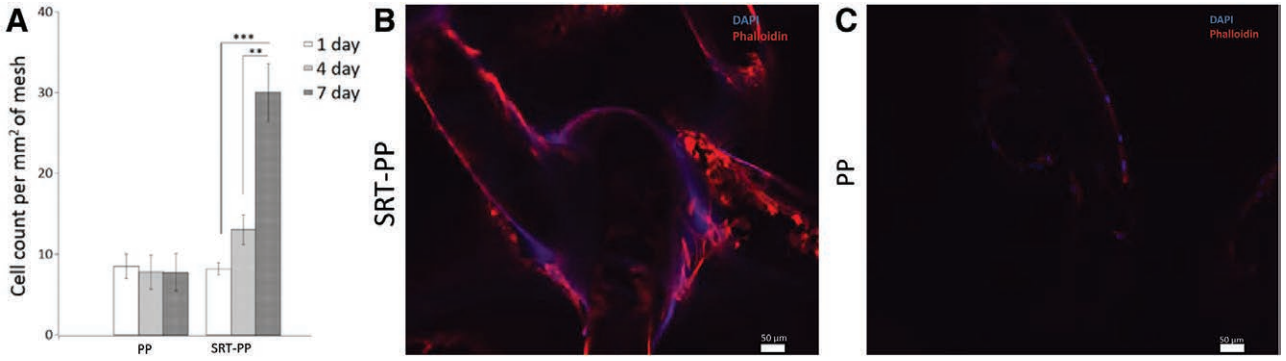

Fig. 2. Cell seeding, count, and adhesion. A, Cells/mm^2 mesh after 1, 4, and 7 days. B, Immunofluorescence with DAPI and Phalloidin of SRT-PP mesh. C, Immunofluorescence with DAPI and Phalloidin of PP mesh. * statistical significance.

any clinical evidence of infection, seroma, or hernia development during the implantation period. MRI of the abdominal cavity for composite and control mesh studies demonstrated no occult seroma or hernia development (**see figure, Supplemental Digital Content 3, which displays MRI,** ***http://links.lww.com/PRSGO/A829***).

Necropsy and Adhesion Scoring

Upon necropsy, we observed that the mesh repair was completely intact in both the SRT-PP and PP control groups. However, the PP group (n = 3) had significant craniocaudal mesh contraction, whereas the SRT-PP group (n = 6) had no contraction (2.27 versus 0.08 cm, $P = 0.05$; Fig. 3A, D). Despite the 3-fold increase in mesh contraction, there was no statistically significant difference in visceral adhesion formation between SRT-PP and PP groups (3.17 versus 3.0, $P = 0.78$; Fig. 3G). This was graded using an accepted method used in previous hernia studies.[16] In the SRT-PP group, 1 rat had grade 2 adhesions, and 1 had grade 5 (colonic serosa was adherent to the mesh), whereas the rest had grade 3 (Fig. 3B, C). All of the control rats had grade 3 adhesions (Fig. 3E, F).

Histology

H&E staining showed chronic lymphoplasmacytic inflammation was identical in both groups (SRT-PP 3.3

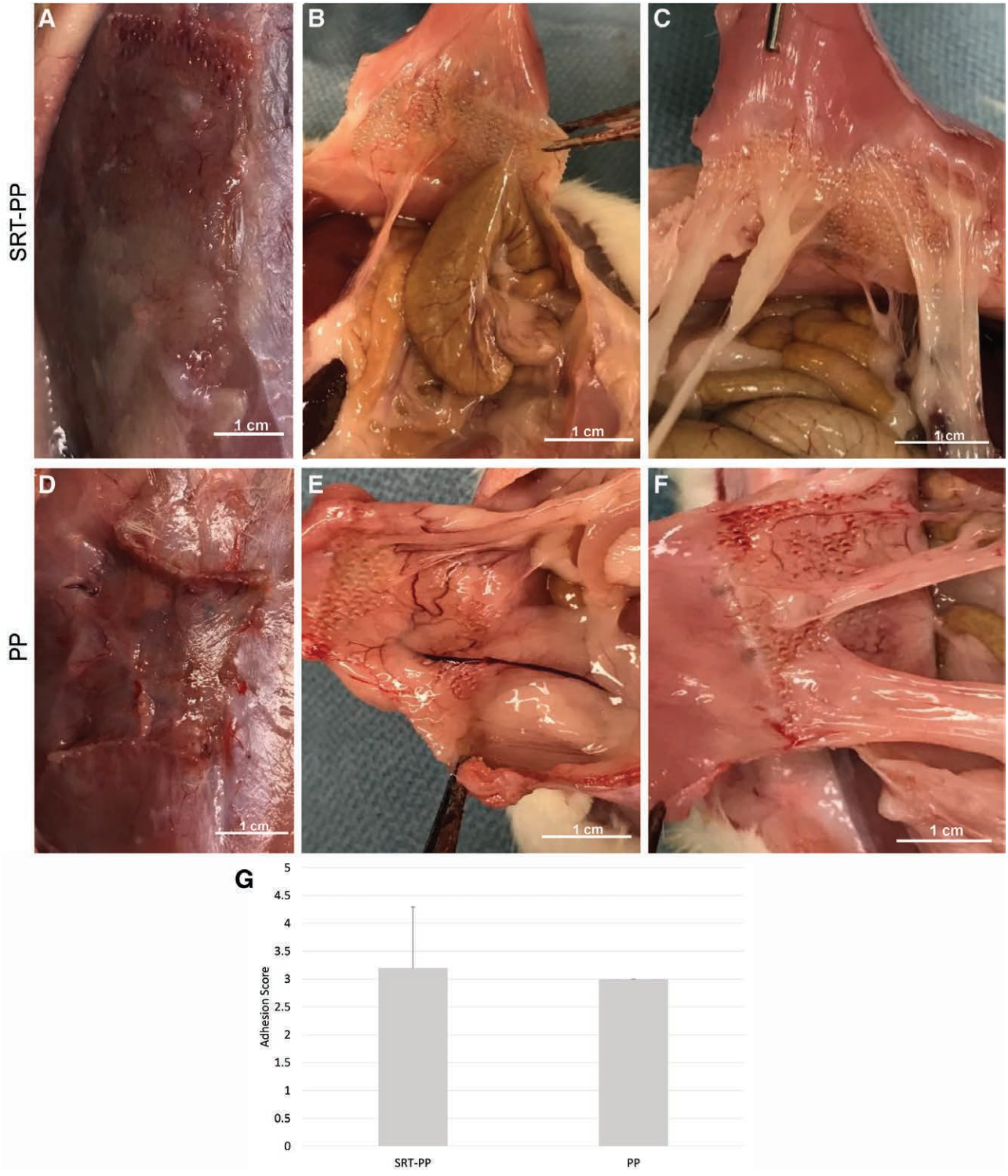

Fig. 3. Necropsy and adhesion scoring. A, SRT-PP rat at necropsy showing no contraction. B, SRT-PP rat with grade 5 adhesion (colonic serosa attached to mesh). C, SRT-PP rat with grade 2 adhesions. D, PP rat at necropsy showing vertical mesh contraction. E and F, PP rats with grade 3 adhesions. G, Qualitative adhesion scores for composite SRT-PP and control PP.

versus PP 3, $P = 0.4$; Fig. 4). Congruent inflammation between groups seemed to indicate a foreign body reaction to the mesh without any adverse effects from the SRT coating. Despite similar inflammation parameters, the SRT-PP group demonstrated increased fibrosis and collagen deposition ventral (toward the skin) to mesh placement as demonstrated on trichrome staining (SRT-PP 168 µm versus PP 52 µm, $P = 0.005$).[19] This was consistent with our in vitro study of cell proliferation where SRT coated meshes were characterized by a 3-fold increase in cell prolifera-

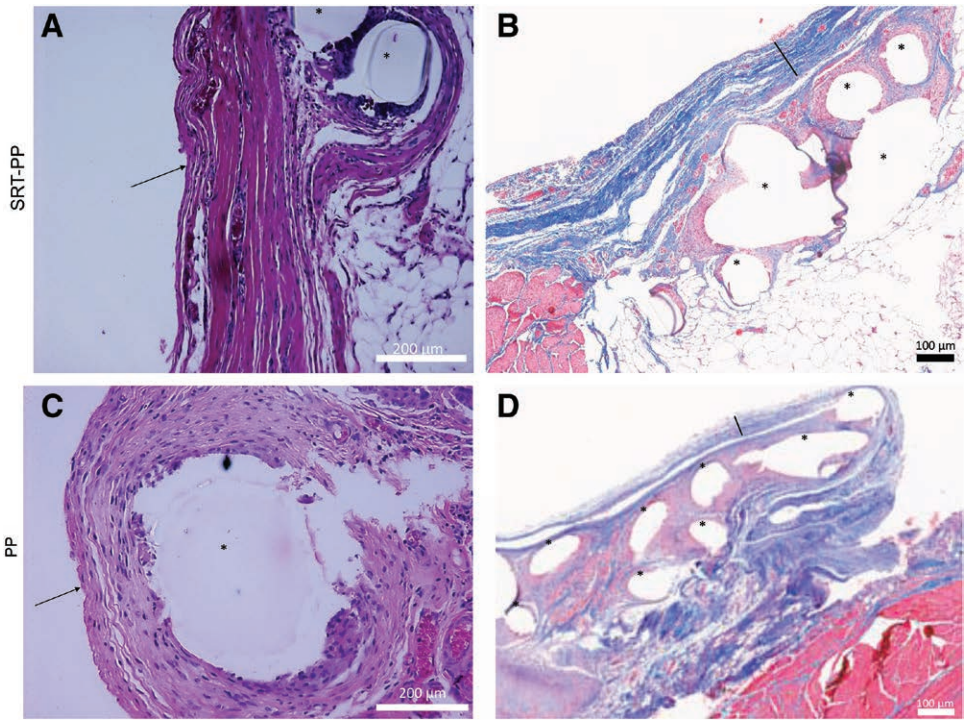

Fig. 4. Histology. A, H&E staining of SRT-PP rat abdominal wall + mesh (40×). B, Trichrome staining of SRT-PP rat abdominal wall+mesh (10×). C, H&E staining of PP rat abdominal wall + mesh (40×). D, Trichrome staining of PP rat abdominal wall+mesh (10×). Arrows pointing to anterior fibrosis, bars (\) showing thickness, and asterisks (*) showing mesh fibers.

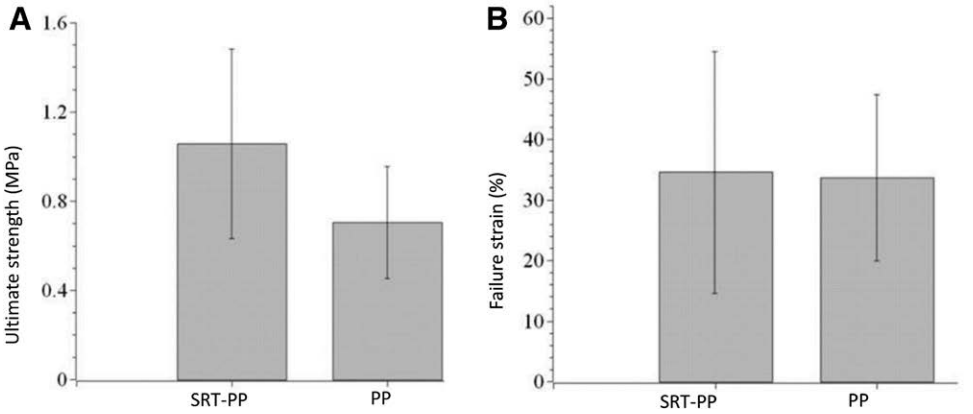

Fig. 5. Biomechanical testing of explants. A, Ultimate strength and (B) Failure strain of tissue explants seized from rats that have composite SRT-PP and control PP mesh.

tion compared with uncoated PP mesh. Liver histology demonstrated normal architecture and no foreign body granulomas (**See figure, Supplemental Digital Content 4, which displays Liver Histology, *http://links.lww.com/PRSGO/A830***).

Biomechanical Testing of Explants

Biomechanical testing of mesh–tissue explants showed that tissue explants from SRT-PP mesh tended toward greater adhesion strength (0.99 MPa versus 0.82 MPa, P = 0.61) than the PP group. Additionally, SRT-PP explants had greater failure strain (41% versus 33%, P = 0.62; Fig. 5) due to increased integration at the mesh–tissue interface (ie, SRT protein coating increases integration). Secondary to the limited number of animals used in this study, these results failed to reach statistical significance.

DISCUSSION

Our study demonstrates that a thin SRT coating appears to increase the strength of the mesh–tissue interface in a bridged abdominal wall repair without any increase in inflammation. SRT binds to abdominal wall proteins, while not relying on the typical inflammatory process of scar formation.[20] High mechanical properties (ie, elastic

modulus of 2–4 GPa and strength of 50–100 MPa) and significantly less craniocaudal shrinkage were seen compared with uncoated PP mesh. These unique properties may allow it to function better than other synthetic and biologic meshes, which can experience significant shrinkage[21] or increased recurrence rates,[22] respectively, as demonstrated in both animal studies and clinically.[23] Mesh shrinkage has been associated with significant postoperative pain in patients.[24] Furthermore, although it failed to reach statistical significance, SRT demonstrated the ability to enhance abdominal wall integration when utilized as a composite coating on PP mesh. Histologically, this appeared as an increase in collagen deposition anterior to the mesh and was corroborated by increased ultimate strength. The collagen-rich scar formation led to the increase in mechanical strength, as has been previously cited for other meshes.[25] These characteristics allowed for similar complication rates, with regard to visceral adhesions, when compared with PP mesh.

Our findings suggest that SRT coating can be used to increase mesh–tissue integration without any significant adverse effects, both locally and systemically. Although the material strength of synthetic mesh is adequate to restore abdominal wall integrity, either a sublay or onlay repair is required to protect the viscera from unwanted inflammatory effects. This leads to a paucity of durable options in patients where fascial reapproximation is not possible. Composite meshes are currently used in this population and typically consist of a PP or polyester base, which are covered with a protective membrane/film to prevent against visceral adhesion or fistula formation.[23] However, by limiting tissue integration, these coatings may limit the strength of the final repair, especially when used in a bridged position as only the mesh periphery has fascial contact. Recurrent mesh failures have led toward the investigation of total abdominal wall transplantation[26] in certain instances. Furthermore, composite meshes have a substantially higher material cost when compared with PP ($2000 versus $250 for 12×8 cm).[27] Biologic meshes are even more costly with prices exceeding $5000 for a similarly sized piece and are prone to recurrences.[22] Therefore, in patients requiring bridged repair, a standalone SRT mesh may have the potential to improve outcomes while minimizing material costs.

Despite promising results of the pilot study, there are several limitations. We used a small rodent model and sample size to demonstrate safety and biocompatibility, which allowed us to keep research costs to a minimum. We recognize that larger animals may offer a better representation of human abdominal wall functionally and are in the planning stages of pig studies. Although PP mesh is not used in a bridged position clinically, we again did not want to incur the high expenses of a composite or biologic material in a first-time animal study. For future studies, we will plan for direct comparisons between an SRT-standalone, SRT-PP, SRT-biologic, synthetic-composite, and biologic mesh. Likewise, future studies will evaluate bridged, sublay, and onlay placement, which will allow for better assessment in all types of abdominal wall repairs that are being done clinically. In addition, some animals will be evaluated for longer time periods to assess for development of enterocutaneous fistulas. Further analyses will include models of abdominal wall component separation where mesh plays a major role in both anterior and posterior approaches.

CONCLUSIONS

This first-time animal pilot study showed that high-strength SRT protein is biocompatible, and its coating on PP does not show increased cellular signs of inflammation above uncoated PP. In addition, composite SRT-PP mesh showed superior abdominal wall integration compared with standard PP mesh. Because SRT is a biologically derived material and provides high strength, it may prove useful in hernia repair. When combined with its relatively low cost of production, it offers potential as a mesh coating, and future studies will evaluate its potential as a standalone mesh material. In either scenario, it may be poised to significantly improve the mesh armamentarium.

Dino J. Ravnic, DO, MPH
Division of Plastic Surgery, Department of Surgery
Penn State University College of Medicine
500 University Drive
Hershey, PA 17033
E-mail: dravnic@pennstatehealth.psu.edu

ACKNOWLEDGMENTS

The authors would like to thank the Turkish Ministry of National Education graduate scholarship (BA) and the International Postdoctoral Research Scholarship Program (BIDEP 2219) of the Scientific and Technological Research Council of Turkey (VO). The authors would also like to thank Aaron Selnick (Penn State University) for helping in extraction of SRT rings, John Reibson (Penn State College of Medicine) for EtO sterilization of mesh, Donna Sosnoski (Penn State University) for her assistance in cell culture, and Dr. Jian Yang, PhD (Penn State University) for providing facilities for mechanical testing of explants, and additionally, Emma Dahmus, MSIII (Penn State College of Medicine) for her assistance in adhesion scoring, Jian-Li Wang, MD, PhD (Penn State College of Medicine) for his assistance in MRI interpretation, and Erik Washburn, MD (Penn State Health) for his assistance in histological assessment.

REFERENCES

1. Holzheimer RG, Mannick JA. *Surgical Treatment: Evidence-based and Problem-oriented*. Munich, Germany: Zuckschwerdt; 2001.
2. Gillion JF, Sanders D, Miserez M, et al. The economic burden of incisional ventral hernia repair: a multicentric cost analysis. *Hernia*. 2016;20:819–830.
3. van Ramshorst GH, Eker HH, Hop WC, et al. Impact of incisional hernia on health-related quality of life and body image: a prospective cohort study. *Am J Surg*. 2012;204:144–150.
4. Beadles CA, Meagher AD, Charles AG. Trends in emergent hernia repair in the United States. *JAMA Surg*. 2015;150:194–200.
5. Vidović D, Jurisić D, Franjić BD, et al. Factors affecting recurrence after incisional hernia repair. *Hernia*. 2006;10:322–325.
6. Breuing K, Butler CE, Ferzoco S, et al. Incisional ventral hernias: review of the literature and recommendations regarding the grading and technique of repair. *Surgery*. 2010;148:544–558.
7. Read RC. Milestones in the history of hernia surgery: prosthetic repair. *Hernia*. 2004;8:8–14.
8. Kaufman Z, Engelberg M, Zager M. Fecal fistula: a late complication of Marlex mesh repair. *Dis Colon Rectum*. 1981;24:543–544.

9. Dwyer PL, Riss P. Synthetic mesh in pelvic reconstructive surgery: an ongoing saga. *Int Urogynecol J*. 2016;27:1287–1288.
10. Basta MN, Fischer JP, Kovach SJ. Assessing complications and cost-utilization in ventral hernia repair utilizing biologic mesh in a bridged underlay technique. *Am J Surg*. 2015;209:695–702.
11. Giordano S, Garvey PB, Baumann DP, et al. Primary fascial closure with biologic mesh reinforcement results in lesser complication and recurrence rates than bridged biologic mesh repair for abdominal wall reconstruction: a propensity score analysis. *Surgery*. 2017;161:499–508.
12. Demirel MC, Cetinkaya M, Pena-Francesch A, et al. Recent advances in nanoscale bioinspired materials. *Macromol Biosci*. 2015;15:300–311.
13. Pena-Francesch A, Domeradzka NE, Jung H, et al. Research update: programmable tandem repeat proteins inspired by squid ring teeth. *APL Materials*. 2018;6:010701.
14. Gaddes D, Jung H, Pena-Francesch A, et al. Self-healing textile: enzyme encapsulated layer-by-layer structural proteins. *ACS Appl Mater Interfaces*. 2016;8:20371–20378.
15. Sariola V, Pena-Francesch A, Jung H, et al. Segmented molecular design of self-healing proteinaceous materials. *Sci Rep*. 2015;5:13482.
16. Deeken CR, Matthews BD. Comparison of contracture, adhesion, tissue ingrowth, and histologic response characteristics of permanent and absorbable barrier meshes in a porcine model of laparoscopic ventral hernia repair. *Hernia*. 2012;16:69–76.
17. Krimm S. Infrared spectra of high polymers. In: *Fortschritte der Hochpolymeren-Forschung*. New York: Springer; 1960:51–172.
18. Jung H, Pena-Francesch A, Saadat A, et al. Molecular tandem repeat strategy for elucidating mechanical properties of high-strength proteins. *Proc Natl Acad Sci U S A*. 2016;113:6478–6483.
19. Calvi EN, Nahas FX, Barbosa MV, et al. An experimental model for the study of collagen fibers in skeletal muscle. *Acta Cir Bras*. 2012;27:681–686.
20. Morch A, Pouseele B, Doucède G, et al. Experimental study of the mechanical behavior of an explanted mesh: the influence of healing. *J Mech Behav Biomed Mater*. 2017;65:190–199.
21. Gruber-Blum S, Brand J, Keibl C, et al. Abdominal wall reinforcement: biologic vs. degradable synthetic devices. *Hernia*. 2017;21:305–315.
22. FitzGerald JF, Kumar AS. Biologic versus synthetic mesh reinforcement: what are the pros and cons? *Clin Colon Rectal Surg*. 2014;27:140–148.
23. Eriksen JR, Gögenur I, Rosenberg J. Choice of mesh for laparoscopic ventral hernia repair. *Hernia*. 2007;11:481–492.
24. Nohuz E, Alaboud M, Darcha C, et al. Effectiveness of Hyalobarrier and Seprafilm to prevent polypropylene mesh shrinkage: a macroscopic and histological experimental study. *Int Urogynecol J*. 2014;25:1081–1087.
25. Schäfer-Nolte F, Hennecke K, Reimers K, et al. Biomechanics and biocompatibility of woven spider silk meshes during remodeling in a rodent fascia replacement model. *Ann Surg*. 2014;259:781–792.
26. Giele H, Vaidya A, Reddy S, et al. Current state of abdominal wall transplantation. *Curr Opin Organ Transplant*. 2016;21:159–164.
27. Reynolds D, Davenport DL, Korosec RL, et al. Financial implications of ventral hernia repair: a hospital cost analysis. *J Gastrointest Surg*. 2013;17:159–166; discussion 166–167.